Dose Optimization for Long-term rAAV-mediated RNA Interference in the Nigrostriatal Projection Neurons

Ayse Ulusoy[1], Gurdal Sahin[1], Tomas Björklund[1], Patrick Aebischer[2] and Deniz Kirik[1]

[1] *Brain Repair and Imaging in Neural Systems, Department of Experimental Medical Science, Lund University, Lund, Sweden;* [2] *Laboratory for the Study of Neurodegeneration, Brain and Mind Institute, Ecole Polytechnique Fédérale de Lausanne (EPFL), Lausanne, Switzerland*

Abstract

Short-hairpin RNA (shRNA)-mediated gene knockdown is a powerful tool for targeted gene silencing and an emerging novel therapeutic strategy. Recent publications, however, reported unexpected toxicity after utilizing viral-mediated shRNA knockdown *in vivo*. Thus, it is currently unclear whether shRNA-mediated knockdown strategy can be used as a safe and efficient tool for gene silencing. In this study, we have generated rAAV vectors expressing shRNAs targeting the rat tyrosine hydroxylase (TH) mRNA (shTH) for testing the efficacy of *in vivo* TH knockdown in the nigral dopaminergic neurons. At high titers, not only the shTH vectors but also the scrambled and green fluorescence protein (GFP)-only controls caused cell death. In a dose-response study, we identified a dose window leading to >60% decrease in TH^+ neurons without any change in vesicular monoamine transporter-2 (VMAT2) expression. Moreover, using the safe and efficient dose, we showed that dopamine (DA) synthesis rate was significantly reduced and this lead to emergence of motor deficits in the shTH-expressing rats. Interestingly, these animals showed very robust and long-lasting recovery after a single systemic L-3,4-dihydroxyphenylalanine (L-DOPA) administration beyond what can be achieved in 6-hydroxydopamine (6-OHDA)-lesioned rats. Our results have implications for both mechanistic and therapeutic studies utilizing long-term shRNA-mediated gene silencing in the nigrostriatal projection system.

Introduction

Gene silencing based on the principle of RNA interference (RNAi) is an emerging powerful technique for knockdown of gene expression in the adult organism.[1,2] Small interfering RNA (siRNA) sequences have the potential to target any gene and could be utilized as a therapeutic tool. Whereas naked siRNAs can be applied for systemic applications and for short-term gene silencing, their use in the central nervous system for long-term gene knockdown has been limited. [3] One of the main challenges for obtaining long-term RNAi-mediated gene knockdown in the brain is the means of delivery as the blood brain barrier generates a limitation for the use of various systemic delivery methods of RNAi in the central nervous system. Therefore studies that required long-term and stable silencing of the target genes in the brain and spinal cord have utilized recombinant viral vectors constitutively expressing either a short-hairpin RNA (shRNA) or an artificial micro RNA (miRNA), which uses the endogenous cellular pathways for RNAi.[4]

Viral vector approaches provide evidence that shRNAs can in fact be used as tools to achieve functional changes in the central nervous system. Tyrosine hydroxylase (TH), the rate-limiting enzyme of dopamine (DA) synthesis, has been silenced in the midbrain dopaminergic neurons in mice using recombinant adeno-associated virus serotype 2 (rAAV2)

giving rise to 36% decrease in the TH mRNA which led to behavioral impairment in amphetamine-induced locomotor activity and reduced performance in the rotarod test.[5] Another study targeting mutant ataxin-1 in a transgenic mouse model of spinocerebellar ataxia type 1 showed that rAAV2-mediated shRNA silencing can lead to substantial decrease of human ataxin-1 expression resulting in motor improvement and normalized cerebellar pathology.[6] Later, in two independent studies, lentiviral vectors were utilized to silence superoxide dismutase (SOD1) expression in a transgenic mouse model of amyotrophic lateral sclerosis overexpressing a mutated form of the human SOD1 gene. Both studies demonstrated that knocking down SOD1 by lentiviral shRNAs delayed the disease progression and extended the survival of the mice. In both studies, treated mice exhibited a significant improvement in motor function supporting the therapeutic potential of shRNA mediated targeted gene silencing.[7,8]

More recently, however, the utility of viral vector-mediated shRNAs for *in vivo* targeted knockdown studies has been questioned due to unexpected toxicity leading to cell death. By using a double stranded rAAV8 vector, Grimm and colleagues observed liver damage and lethality after expression of shRNAs targeting the human α-1 antitrypsin mRNA in a transgenic mouse line.[9] They found that toxicity was associated with downregulation of endogenous miRNAs, which could be eliminated by reducing the viral titer. These findings led them to conclude that high levels of shRNA expression could saturate the RNAi pathway in the cell causing unwanted side effects and toxicity. On the other hand, striatal toxicity observed after rAAV1 shRNA delivery to silence the mutant huntingtin expression in the CAG140 knock-in mouse model of Huntington's disease was found not to be related to the saturation of the miRNA pathway.[10] In fact, the latter study reported that although the diluted vector resulted in reduced transduction efficiency in the striatum, it did not decrease the toxicity. Thus, it presently remains unclear whether a dose window for viral vector mediated shRNA expression that does not lead to non-specific toxicity but maintains high efficacy *in vivo* in the brain can be defined.

Results

In this study, our aim was to test whether it is possible to achieve an efficient and long-term knockdown of the TH expression in rat substantia nigra (SN) by continuous expression of shRNA constructs from an rAAV5 vector without causing any nonspecific toxic effects in the transduced cells. For this purpose, we generated rAAV5 vectors expressing two different knockdown constructs and their scrambled controls. An initial set of 10 siRNA was designed according to the Tuschl rules.[11] Using an expression cassette driven by the H1 promoter, the resulting silencing efficacy was tested by co-transfection with the enhanced green fluorescence protein (GFP)-rat TH fusion protein–expressing plasmid in 293T cells. Expression of the GFP-rat TH fusion protein was monitored by flow cytometry and the final two sequences were selected for maximal silencing efficacy. The *in vivo* work included a dose–response study for rAAV5 vectors expressing both active shRNA vectors (shTH1 and shTH2) and their scrambled controls (shTH1scr and shTH2scr). To be able to identify the transduced cells unambiguously, all rAAV5 vectors expressed GFP driven by a synthetic chicken β-actin promoter. In addition, a separate rAAV5 vector coding only for the GFP marker gene was used as a non-shRNA control vector. Our goal was to define a dose window that would result in an efficient knockdown without causing toxicity. The level of knockdown was assessed in histological specimens by quantifying the number of nigral neurons expressing TH, whereas reduction in vesicular monoamine transporter-2 (VMAT2)-expressing cells was used as a measure of nonspecific toxicity.

High level of gene expression in the SN can lead to toxicity

Seven weeks after unilateral transduction by rAAV5 vectors, the animals were killed and the brains were processed for histological analysis followed by stereological estimation of phenotypic markers of the DA neurons in equally spaced sections covering the entire SN. The vector titers injected in each group was varied 2–3 orders of magnitude covering the range 10^9 to 10^{13} genome copies (gc)/ml with titer matching groups from 10^{10} to 10^{12} gc/ml across the different vector preparations (**Figure 1**). To determine the extent of the specific TH knockdown in the nigral dopaminergic neurons, we performed stereological estimation of total TH^+ and $VMAT2^+$ cell numbers in adjacent series in all animals (**Table S1**). Whereas TH cells were expected to be reduced after treatment with the active shRNA constructs (shTH1 and shTH2), reduction in $VMAT2^+$ cells in this group or any significant change in either the TH^+ or the $VMAT2^+$ cells in the control groups (shTH1scr, shTH2scr, or GFP-only) would indicate nonspecific effects. Indeed, delivery of rAAV5-shTH1 at 2.8×10^{12} gc/ml and rAAV5-shTH2 vector at 3.7×10^{12} gc/ml led to 85% and 92% decrease in the number of nigral TH^+ neurons compared to the intact side of the same animal (**Figure 1a,d**).

Quantification of $VMAT2^+$ cells in the same groups, however, revealed a significant decrease as well. The reductions in the $VMAT2^+$ neurons were about 37% and 55% in the nigra of the rAAV5-shTH1 and rAAV5-shTH2 injected animals, respectively. This suggested that while there was an effective knockdown of the specific target, at these doses, the treatment also led to measurable toxicity *in vivo*. Moreover, a similar level of toxicity was also present in the SN of the animals injected with rAAV5 vectors expressing the scrambled control sequences, shTH1scr and shTH2scr, as well as the GFP-only group when vector titers higher were at or higher than low 10^{12} gc/ml. The toxicity was seen as a 37–43% reduction in both TH^+ and $VMAT2^+$ cell numbers, which was not only statistically but also biologically significant unwanted outcome (**Figure 1b,c,e**).

Optimal shRNA expression levels lead **leads to robust knockdown without apparent toxicity**

Next, we asked the question whether the toxicity was dose related and if so would there be a window within which the efficiency of the specific knockdown could be maintained but the nonspecific effects were greatly reduced or eliminated. For this purpose, we carried out the same analysis as above and compared the $VMAT2^+$ and TH^+ cell numbers in the SN using lower titers of all five rAAV5 vectors. The results from the estimations of total cell numbers showed that rAAV5-shTH1 was not toxic at titers below 1.4×10^{12} gc/ml, as concluded by the presence of normal constituent of $VMAT2^+$ cells. Importantly, the efficiency of knockdown in the nigral dopaminergic neurons using this construct was maintained at above 60% at a titer range between 1.8×10^{11} and 1.4×10^{12} gc/ml (**Figure 1a**). rAAV5-shTH2 expression on the other hand, caused toxicity even at 7.8×10^{11} gc/ml, which was not present at 2.0×10^{11} but at the latter dose the knockdown efficiency was found to be only about 50% (**Figure 1d**). Nonspecific effects seen with the scrambled sequences or the GFP vectors were also eliminated in the groups that were injected at vector titers within the 10^{11} to 10^{12} range (**Figure 1b,c,e**). The specific knockdown of the TH expression using the shTH1 construct and its comparison to the titer-matched shTH1scr control is illustrated at four levels in the rostrocaudal axis (**Figure 2a–d** and **Figure 2m–p**, respectively). The adjacent sections stained with VMAT2 are shown for comparison (**Figure 2e–h,q–t**). The efficiency of the transduction

can also be illustrated using the GFP expression in the same animals as these transfer plasmids were designed to coexpress this marker gene (**Figure2i–l,u–x**).

We next performed a triple immunohistochemical staining against TH, VMAT2, and GFP for animals injected with mid 10^{11} gc/ml titers of rAAV5 vectors expressing shTH1, shTH1scr, or GFP-only and conducted confocal microscopy on the triple-labeled samples to demonstrate the localization of these markers. On the intact side, both TH and VMAT2 were well expressed in the SN pars compacta (**Figure3a,b**) and were colocalized in all cells (**Figure 3d**). In the nigra of the animals injected with the rAAV5-shTH1 vector, on the other hand, TH protein was efficiently downregulated to levels below detection limits of laser-scanning confocal microscopy (**Figure 3e**), while VMAT2 remained unchanged (**Figure 3f**). Due to the fact that the same vectors also expressed GFP, we were able to document the presence of GFP^+ / $VMAT2^+$ but TH-negative neurons illustrating TH knockdown in the nigral DA neurons (**Figure3e–h**). Neither the shTH1scr nor the GFP-only control vectors yielded any TH knockdown (**Figure3i** and **Figure 3m**, respectively). Thus in these animals all three markers were colocalized (**Figure3l,p**).

In order to confirm that low 10^{11} gc/ml titers of rAAV5 vectors expressing all three constructs did not cause any cytotoxicity, we performed immunohistochemical stainings against the neuronal marker Hu and the microglial marker Iba1, as well as Nissl staining using cresyl violet (**Figure 4)**. At the optimal dose range determined here, we found no apparent change in Hu^+ neurons in the transduced SN of animals treated with rAAV vectors expressing GFP, shTH1scr, or shTH1 (**Figure 4d,g,h**) as compared with the uninjected intact side of the brain (**Figure 4a)**. This was associated with a normal cytoarchitechture and cellular density in Nissl stained specimens (**Figure 4f,i,l;** compared with **Figure 4c**), and the appearance of resting microglia (**Figure 4e,h,k** compared with **Figure 4b**). However, all animals injected with high doses of vectors leading to neurotoxicity demonstrated a significant clearance of Hu^+ neurons in the SN pars compacta (**Figure 4m**), which was associated with microglial activation around the injection area and in several cases more widely throughout the nigra (**Figure 4n**), as well as hypercellularity and vascular cuffing suggesting severe inflammatory response to the treatment (**Figure 4o**).

Optimal dose of rAAV5-shTH1 expression leads to a selective decrease in TH enzyme activity and behavioral impairments that can be reversed by L-DOPA

To test the functional consequences of TH knockdown in the rat SN, two additional groups of animals were injected with 1×10^{11} gc/ml rAAV5-shTH1 (n =7) or 3.4×10^{11} gc/ml rAAV5-shTH1scr (n = 9). A third group of animals (n = 9) that received three-site striatal 6-hydroxydopamine (6-OHDA) injections were included as lesion-reference group, while nontreated rats (n = 6) served as intact controls. We performed a microdialysis study 9-12 weeks after the vector injection. The animals were given an intraperitoneal injection of an aromatic L-amino acid decarboxylase (AADC) enzyme inhibitor NSD-1015 to block the conversion of endogenously synthesized 3,4-dihydroxyphenylalanine (DOPA) to DA. The rate of accumulation of DOPA, providing a measure of the activity of TH enzyme *in vivo*, was significantly lower in shTH1 and 6-OHDA groups compared to the intact animals, whereas no significant difference was observed in shTH1scr group (**Figure 5a**). DOPA synthesis rate measured between 0 and 90 minutes was 5.3 fmol/minute in rAAV5-shTH1-treated animals representing 66 and 70% reduction as compared to the scrambled and intact controls, respectively (**Figure 5b**). Similarly, the in vitro TH enzyme activity measured from the striatal

tissue extracts confirmed that TH activity was reduced by about 63% in shTH1 group and 70% in the 6-OHDA lesion group compared to the intact side values, whereas the results from scrambled controls did not differ from the intact rats (**Figure 5c**). To illustrate the specificity of the TH knockdown, we have, in addition, measured the AADC enzyme activity from the same tissue samples. As expected dopaminergic neurodegeneration in the 6-OHDA lesion group caused a corresponding reduction also in the AADC enzyme activity. On the contrary, AADC activity remained unchanged in shTH1 and shTH1scr groups compared to the intact animals, confirming the specificity of the knockdown (**Figure 5d**).

To further confirm that rAAV-mediated shTH1 expression leads to functional changes in the transduced DA neurons, a cylinder test was performed 7 weeks after surgery. The animals were tested for forepaw use bias in the cylinder test. We found 23% decrease in the left forepaw use in the shTH1 group, whereas the expression of the shTH1scr construct had no apparent behavioral effect, similar to intact control rats. As expected, the 6-OHDA lesioned animals showed a clear impairment in this test and used the left forepaw in about 10% of the wall touches.

We then treated these animals with a single treatment of systemic L-DOPA at a dose of 6 mg/kg to confirm that the behavioral impairment observed in shTH1 group is caused by DA deficiency and that it was reversible. The cylinder test was repeated again at 90, 180, and 360 minutes after L-DOPA treatment. There was a complete recovery in the shTH1 group already at 90 minutes, which was maintained for at least 6 hours. The same dose of L-DOPA, on the other hand, provided a minor change (from 10% to 21%) in the 6-OHDA-lesioned rats at 90 minutes, which returned to baseline already at 180 minutes (**Figure 6**).

Discussion

In this study, we demonstrated that long-term efficient knockdown of TH in the absence of any apparent nonspecific toxicity can be obtained using an rAAV-mediated shRNA delivery. For this purpose, we utilized a dose–response study design and targeted the nigral DA neurons to silence the expression of the TH protein, the rate-limiting enzyme in DA synthesis. We tested two rAAV5 vectors expressing different shRNAs designed to recognize the rat TH mRNA and used scrambled sequences as controls for each functional shRNA construct. These vectors carried also the GFP gene to be able to visualize the virus transduction at the injected area. In addition, we used a third control vector expressing only the GFP gene in order to tease out whether any toxic effects that might be seen in the above constructs were shRNA specific. We found that the rAAV5 viral vectors could lead to nonspecific toxicity when delivered at high titers but that this toxicity was similar to what is seen after the injection of GFP-only control vector suggesting that the phenomenon was unlikely to be a result of the shRNA expression. At any rate, dilution of the vector stocks to titers in the low-mid 10^{11} gc/ml resulted in disappearance of toxicity. The efficacy of the knockdown, on the other hand, still remained at >60% as assessed by TH^+ cell numbers and TH enzyme activity measurements *in vivo* and in vitro suggesting that a therapeutic window for specific knockdown in the nigral DA neurons was feasible after viral vector-mediated expression of shRNA constructs.

The analysis of dose-response data in this experiment relied on the immunohistochemically stained paraformaldehyde-fixed brains. Although the quantification of cells stained for a marker protein does not allow for precise quantification of the efficacy of the shRNA-mediated knockdown of the target protein, the very same analysis is a robust

means to achieve differential assessment of specific knockdown versus nonspecific effects, in our case, also leading to cell loss. Indeed, we took advantage of the fact that the nigral DA neurons express multiple phenotypic markers. Whereas the TH enzyme was the target for the shRNA-mediated knockdown, we utilized VMAT2, the specialized transporter that handles the vesicular storage of DA, as the second marker protein. In addition, we confirmed that the decrease in $VMAT2^+$ cell numbers in high titer vector injections correlated with another neuronal marker, Hu, illustrating that the decrease in VMAT2 staining was not due to unexpected, secondary downregulation of the VMAT2 protein, but rather cell loss. Thus, comparative analysis of $VMAT2^+$ and TH^+ cell numbers in the SN allowed us to distinguish genuine knockdown versus cell death. This analysis helped to establish a working dose range of the specific shRNA-expressing vector leading to sufficient knockdown of the target mRNA without any apparent toxicity. Moreover, as the viral vectors also expressed the GFP marker gene along with the shRNA for TH, we could utilize triple immunohistochemistry for TH, VMAT2, and GFP in the same specimen to demonstrate that a $TH^+/VMAT2^+$ DA neuron could be converted to a $TH^-/VMAT2^+/GFP^+$ cell after transduction.

As the virus injections were performed unilaterally, the asymmetry in forepaw use could be used as a measure for behavioral impairment. To further confirm the specificity of the optimal dose window obtained by the immunohistochemistry data we performed cylinder test in a separate group of animals injected with low 10^{11} gc/ml rAAV5 expressing shTH1 and shTH1scr. As expected, TH knockdown caused about 50% decrease in affected (left) paw use and this impairment could be reversed completely by L-DOPA injection suggesting that the behavioral impairment is caused by the decrease of DA. Interestingly, contrary to the 6-OHDA lesioned group, L-DOPA injections provided a robust recovery that lasted >6 hours in the shTH1 group showing that although these animals had an impaired DA synthesis, they retained the capacity to convert exogenously administered L-DOPA to DA and store DA in the vesicles due to structural integrity of the pre-synaptic DA terminals in the striatum ipsilateral to the injection. Further proof to this effect was provided by analysis of the activity of TH enzyme in an *in vivo* microdialysis experiment, as well as in vitro TH and AADC enzyme activity assays performed in striatal tissue extracts.

We used two different shRNA sequences targeting the TH mRNA for our *in vivo* studies in which both constructs led to robust TH knockdown but also caused significant cell loss in the nigral dopaminergic neurons after injection of high titer vectors. Although our aim was not to investigate the exact cause of toxicity, the cell loss triggered by injecting rAAV vectors expressing shRNA could be interpreted as a result of an off-target knockdown of other mRNAs or saturation of the miRNA pathway. Alternatively, the toxicity could be a result of a nonspecific effect due to overdosing, which could be seen with overexpression of any transgene and not related to the shRNA constructs. The fact that not only the high titer shTH1scr and shTH2scr scrambled controls but also the GFP-only group manifested cell death suggests that the latter explanation is more likely to be the case in the present experiment. In support of the above, we observed increased microglial activity and hypercellularity in high titer virus injections, which was independent of the transgene.

Several studies have been performed utilizing viral-mediated *in vivo* gene knockdown using shRNA constructs for central nervous system applications. Using this tool, it has been possible to silence a mutant variant of SOD1 gene leading to a familial form of amyotrophic lateral sclerosis,[7,8] or polyglutamine expansion disease.[6,10,12-14] In another series of experiments, rAAV vectors were used to target expression of normal endogenous proteins

to study loss of function effects in the hypothalamus,[15-17] or midbrain.[5,18,19] However, most of these studies did not report any systematic and quantitative measurements to determine whether or not these experimental manipulations led to any nonspecific toxicity in the transduced tissue. Although relative house-keeping genes or proteins have been reported in some of the studies cited above implicating absence of nonspecific effects, these analyses are not sufficient to conclusively demonstrate lack of cellular toxicity. Moreover, in most cases these analyses were performed from samples taken at relatively short term (2-4 weeks) after transduction. Thus the long-term consequences of the treatment remained by and large unexplored.

Two recent studies, on the other hand, draw attention to viral vector-mediated *in vivo* shRNA toxicity. First, Grimm et al. showed that shRNA-mediated knockdown of human α-1 antitrypsin gene expression in the liver caused hepatotoxicity. Through an extensive series of experiments, they concluded that the toxic effects were due to oversaturation of the miRNA pathway and that the toxicity can be mitigated by diluting the vector while retaining the efficacy of the knockdown.[9] More recently, McBride *et al.* found that rAAV-mediated expression of shRNA against the huntingtin mRNA caused toxicity after injection into the striatum, which was illustrated as loss of DARPP-32 expression and microglial activation at the injection site.[10] They argued that in their case this was due to the presence of high levels of unprocessed antisense RNAs subsequently causing off-target silencing. Contrary to the previous report by Grimm et al.,[9] diluting the vector in this experiment led to reduced transduction without eliminating the toxicity. Interestingly when shRNAs were replaced with an artificial miRNA expression cassette the very same knockdown sequences did not cause toxicity suggesting that artificial miRNAs could provide a better tool for targeted gene silencing studies *in vivo*. [10] Similar results were in fact reported by Rodriguez-Lebron *et al.* where one of the two shRNA constructs targeting htt caused reduction in DARPP-32 and pre-, pro-enkephalin mRNA levels.[13] In a follow-up study, the same group showed that the toxicity seen in their experiment was due to unintended targeting of other mRNAs, rather than potential mechanisms involving the endogenous RNAi machinery.[20] Our findings are in line with those of Grimm *et al.* and suggest that it is possible to eliminate the toxicity but maintain specific knockdown by using the appropriate dilution of the vector. We found that the shTH1 construct could provide >50% knockdown already at 2.2×10^{10} gc/ml titer and >75% knockdown at 1.8×10^{11} gc/ml, while the toxicity was observed only at 3.7×10^{12} gc/ml or higher titers. Thus, the dose window providing only specific affects in as in our case could be as wide as 100-fold titer range. It should be noted, however, that the dilution of the vector in individual cases might reveal variable results leading to suboptimal knockdown efficiency at nontoxic levels, as was observed here using the shTH2 construct. This argues that beyond the selection of the initial predicted siRNA sequences, typically done using an in vitro assay, an *in vivo* titration should also be performed. Thereafter, a secondary selection based on *in vivo* biological results can be conducted to determine an optimal dose for the final selected construct.

An *in vivo* model where DA synthesis capacity can be manipulated in a targeted manner has several important implications for research in Parkinson's disease. First, DA toxicity has long been hypothesized as an important pathogenic mechanism leading to disease, but direct evidence for involvement of DA, e.g., via generation of toxic α-synuclein species has not yet been demonstrated in an *in vivo* system. The viral vector approach combining overexpression and gene knockdown strategies will be powerful tools for such critical proof-of-concept experiments. Second, in the model system described here the DA

synthesis capacity is reduced but structural integrity of the presynaptic terminal site is maintained. This combination could be a unique tool to dissect out pre- versus postsynaptic abnormalities leading to maladaptive plasticity in the DA-depleted striatum. All other lesion models create postsynaptic abnormalities by causing disruption of the presynaptic elements, thus making it impossible to dissociate one aspect from the other. Last, but not least, in order to test the therapeutic potential of RNAi delivery for treatment of PD, safe and effective delivery tools that can provide long-term silencing are critical. The present results show that this requirement can be met with shRNA sequences delivered via an rAAV5 vector provided that proper dose–response studies are performed.

Materials and Methods

Design and construction of the shRNA. A set of 10 siRNA sequences against rat TH was designed according to the Tuschl rules.[11] Sequences for expression of the corresponding shRNAs were subcloned in the pSuper vector between the BglII and HindIII sites. Silencing efficacy was determined by transient co-transfection of each the pSuper-TH shRNA construct with the pGFP-ratTH plasmid in 293T cells. This plasmid was obtained by a subcloning BamHI/XbaI of the rat TH complementary DNA (obtained by reverse transcription-PCR from PC12 cells) into the pGFP-EK vector. The resulting GFP-ratTH fusion protein was expressed under the control of the cytomegalovirus promoter and measured by flow cytometry. For each of the pSuper-TH shRNA constructs, the resulting silencing efficacy was determined with regard to a co-transfection of pGFP-ratTH with an empty pSuper vector. Based on the results obtained in in vitro tests, two functional TH knockdown shR-NAs matching the rat TH at 790–810 (shTH1) and 1284–1303 (shTH2) locations and the corresponding scrambled shRNA duplexes (denoted as shTH1, shTH1scr, shTH2, and shTH2scr, respectively) were selected for *in vivo* use. The sequences for these shRNAs were as follows: shTH1 (5′-aacggtactgtggctaccgagttcaagagactcggtagccacagtaccgtt-3′), shTH1scr (5′-gcgcgtcagtcaggtacagatttcaagagaatctgtacctgactgacgcgc-3′), shTH2 (5′-gatcaaacctaccagcctgttcaagagacagg-ctggtaggtttgatctt-3′), and shTH2scr (5′-gacgcaatcacctgctacattcaagagatgtagca-ggtgattgcgtctt-3′).

Generation of the transfer plasmids for vector production. The two most efficient active sequences (shTH1 and shTH2) and their scrambled controls (shTH1scr and shTHscr2) were cloned into an AAV transfer vector in two steps. First, the shRNA sequences were cloned downstream of the H1 promoter. In the second step, *Xho*I–*Sac*I fragments containing the H1-shRNA sequences were cloned into the pTR-UF11 backbone plasmid containing the AAV2 inverted terminal repeats. The insertion was carried out by removing PYF441 enhancer and HSV-tk promoter driven NeoR gene on the original backbone plasmid (pTR-UF11), which was downstream of GFP driven by a cytomegalovirus enhancer hybrid chicken β-actin promoter. The parent plasmid was used for the production of the GFP control vectors without any modifications.

Production of rAAV5 vectors. 293T cells were grown in cell factories (Nunc, Roskilde, Germany) to about 70–80% confluency. The transfection was carried out using the calcium-phosphate method and included the appropriate transfer plasmid (as detailed above) and the pXYZ5 packaging plasmid, encoding for the AAV5 capsid proteins in trans.[21,22] 2.5 mg of DNA with equimolar amounts of helper and transfer DNA was used to transfect the 293 cells. Transfected cells were incubated for 3 days before being harvested by phosphate-buffered saline (PBS)–EDTA. The cell pellet was treated with a lysis buffer (50 mmol/l Tris, 150 mmol/l NaCl, pH 8.4) and lysed by performing three freeze–thaw cycles in dry ice/ ethanol bath. The lysate was then treated with 21 U/ml benzonase (Sigma, Stockholm, Sweden) for nuclear digestion. The crude lysates were purified first by ultracentrifugation (1.5 hours at 350,000g at 18 °C) in a discontinuous iodixanol gradient, and then by ion-exchange chromatography using fast protein liquid chromatography. Briefly, a Q sepharose 5-ml High Trap column (GE Healthcare, Buckinghamshire, UK) was equilibrated by first a low salt concentration buffer

(20 mmol/l Tris, 15 mmol/l NaCl, pH 8.5) then a high salt concentration buffer (20 mmol/l Tris, 500 mmol/l NaCl, pH 8.5). Before initiating the purification, the equilibration was finished by diluting the virus suspension with low salt concentration buffer in the ratio 1:1. The virus was eluted from the column using the high salt concentration buffer previously used for equilibration. The virus suspension was then concentrated using a concentrator (Millipore Amicon Ultra 100-kd molecular weight cutoffs; Millipore, Solna, Sweden) at 1,500*g* and 18°C in two consecutive steps by adding lactated ringer.

The titers of purified viral stocks and all diluted preparations were determined separately using TaqMan quantitative PCR. For this purpose 4 µl of the vector solution was diluted with 16-µl rAAV dilution buffer containing 10 µg/ml salmon sperm DNA and treated with 20-µl of 2 N NaOH for 30 minutes at 56 °C. The lysate was then neutralized using 20-µl of 2 N HCl. For the PCR reaction lysates were diluted 100- fold. Primers and probes were targeted to cytomegalovirus immediate early enhancer (sense: 5′- cgtcaatgggtggactatttacg-3′antisense: 5′-aggtcatgtactgggcataatgc-3′ and probe: 5′-agtacatcaagtgtatcatatgccaag-tacgccc-3′; 5′-fluorescein amidite/3′black hole quencher1). In order to perform an absolute quantification, an rAAV backbone plasmid carrying the cytomegalovirus enhancer hybrid chicken β-actin promoter (pTR-UF20) was linearized with *Hind*III restriction enzyme and purified with a PCR purification kit (Qiagen, Solna, Sweden) according to the manufacturer's instructions. A standard 40-cycle TaqMan PCR amplification was employed for the virus titration and the quantities were calculated using 10-fold serial dilutions of chicken β-actin standards. The final titers for rAAV5 vector stocks coding for shTH1, shTH2, shTH1scr, shTH2scr, and GFP were 3.7×10^{12}, 2.8×10^{12}, 3.6×10^{13}, 2.0×10^{12},and 3.3×10^{13} gc/ml, respectively. For *in vivo* applications, all vectors were diluted in order to have 5–6 doses from the stock titer to 10^9 or low 10^{10} gc/ml, which provides a sufficient range and number of steps for a dose–response study design.

Stereotaxic surgeries. Young adult female Sprague Dawley rats weighing 225–250 g were obtained from Charles River (Kisslegg, Germany). Surgical procedures were performed under either 2% isoflorane gas anesthesia or 20:1 mixture of fentanylcitrate (Fentanyl) and medetomidin hydrochloride (Dormitor) (Apoteksbolaget, Stockholm, Sweden), prepared as an injectable anesthesic. rAAV5 vectors were injected unilaterally into SN using 5-µl Hamilton syringe fitted with a glass capillary with a tip diameter of about 60-80 µm. Two microliters of the buffer containing the appropriate concentrations of viral particles was injected at a speed of 0.4 µl/minute. The needle was withdrawn slowly 5 minutes after completion of the injection. Coordinates used for SN injections were anterioposterior: −5.2 mm and mediolateral: − 2.0 mm relative to the bregma and dorsoventral: − 7.2 mm from the dural surface, according to the atlas of Paxinos and Watson.[23] The tooth bar was adjusted to −2.3 mm in all nigral injections. The 6-OHDA lesions were placed into the right striatum by injecting a total of 21-µg 6-OHDA dissolved in ascorbate-saline (0.05%) delivered in three deposits in the rostrocaudal axis. The coordinates were anterioposterior: +1.0, −0.1, −1.2 mm and mediolateral: − 3.0, −3.7, −4.5 mm relative to the bregma and dorsoventral: − 5.0 mm from the dural surface. The tooth bar was set to 0.0 mm. A volume of 2µl per site was injected at a rate of 1µl/minute. The needle was left in place for 5 minutes after completion of each injection.

Histological analysis. For the histological analysis a total number of 137 animals injected with rAAV5 vector stocks coding for shTH1, shTH2, shTH1scr, shTH2scr, and GFP as well as their dilutions were used. Rats were deeply anesthetized with 1.2 ml sodium pentobarbital (Apoteksbolaget) and then perfused through the ascending aorta with 50 ml physiological saline at room temperature, followed by 250 ml ice-cold 4% paraformaldehyde for 5–6 minutes. Brains were postfixed in 4% paraformaldehyde solution for 2 hours before being transferred into 25% sucrose solution for cyroprotection, where they were kept until they had sunk (typically 24–48 hours) The brains were then sectioned in the coronal plane on a freezing microtome at a thickness of 35 µm. Sections were collected in six series and stored at −20 °C in a phosphate buffer containing 30% glycerol and 30% ethylene glycol until further processing.

Immunohistochemical stainings were performed on free-floating sections. For this purpose, brain sections were first rinsed with potassium-PBS (KPBS), and then endogenous peroxidase activity was quenched in 3% H_2O_2 and 10% methanol in KPBS for 10–30 minutes. After a series of rinsing steps in KPBS, nonspecific binding sites were blocked by incubation in KPBS containing 5% normal serum (from the same species as the corresponding secondary antibody was raised) and 0.25% Triton-X. Samples were then incubated overnight at room temperature in primary antibody solution containing 5% serum and 0.25% Triton-X. The primary antibodies used for immunohistochemical staining were as follows: mouse anti-TH (working dilution 1:2,000, MAB318; Millipore), chicken anti-GFP (working dilution 1:5,000, AB16901; Millipore), rabbit anti-Iba1 (working dilution 1:1,000, 019-19791; Wako, Neuss, Germany), mouse anti-Hu (working dilution 1:250; A-21271, Molecular Probes, Eugene, OR), and rabbit anti-VMAT2 (working dilution 1:1,000, AB1767; Millipore). On the second day, the sections were rinsed in KPBS and then incubated for 1 hour at room temperature in 1:200 dilution of biotinylated secondary antibody solutions horse anti-mouse (Vector Laboratories, Jarfalla, Sweden) for TH and Hu antibodies, rabbit anti-chicken (Promega, Stockholm, Sweden) for GFP antibody and goat anti-rabbit (Vector Laboratories) for Iba1 and VMAT2 antibodies. After rinsing, the sections were treated with avidin–biotin–peroxidase complex (ABC Elite kit; Vector Laboratories) and the color reaction was developed by incubation in 25 mg/ml 3,3′-diaminobenzidine and 0.005% H_2O_2. Sections were mounted on chrome-alum coated glass slides, dehydrated, and cover-slipped with DPX mounting media (Sigma). Cresyl violet stainings were performed on sections mounted on chrome-alum coated glass slides. The slides were passed through a series of alcohol and xylene baths for delipidation, then rehydrated, and treated with 0.5% cresyl violet in 10% acetic acid solution for 4 minutes. After dehydrating the cresyl violet stained specimens, the slides were cover-slipped with DPX mounting media.

For TH, GFP, and VMAT2 triple immunohistofluorescence was carried out as above with the exception that the biotinylated secondary antibodies were replaced with fluorophore conjugated variants (Jackson Immunoresearch, Gothenburg, Sweden) and the H_2O_2 quenching step was excluded. The sections were directly mounted on glass slides and cover-slipped using polyvinyl alcohol-1,4-diazabicyclo[2.2.2]octane (Sigma). The triple immunohistochemical staining was visualized on a Leica DMRE laser-scanning confocal microscope equipped with green helium/ neon, helium/neon, and argon lasers (Leica, Kista, Sweden). The images were taken as z-stacks of six focal planes in sequential acquisition mode, from within the 6–8 μm from the surface of the section. The figures were prepared using the average projection tool in ImageJ software platform (version 1.40g; National Institutes of Health, Bethesda, MD).

Stereological analysis. The estimations of the TH^+ and $VMAT2^+$ cell numbers in the SN were made using an unbiased stereological quantification methods by employing the optical fractionator principle.[24] Although a formal blinding process was not employed, the sections were numbered without any notification of the identity of group, vector type, or dilution. Upon completion of the quantification of batches of samples were moved to a database for further analysis at a later time point using appropriate statistical and graphical tools. The borders for the region of interest was defined by using a ×4 objective, whereas the actual counting was performed using a ×60 Plan-Apo oil objective (numerical aperture = 1.4) on a Nikon 80i microscope equipped with an X–Y motorized stage (Märzhauser, Wetzlar, Germany), a Z-axis motor and a high-precision linear encoder (Heidenhain, Traunreut, Germany). All three axes and the input from the digital camera were controlled by a PC computer that carried out the procedure with a random start systematic sampling routine (NewCast Module in VIS software; Visiopharm A/S, Horsholm, Denmark). The sampling interval in the X–Y axis was adjusted so that at least 100 cells were counted for each SN. The penetration of each antibody was determined by registering the Z-axis position of all counted profiles and plotting a frequency distribution in that axis. This analysis revealed an incomplete staining in the central 4-5 μm part of the sections in TH-stained material and a staining throughout the whole thickness of the sections for VMAT2.[25] The counted volume in TH-stained specimens thus excluded the insufficiently stained

central portion of the sections. Coefficient of error attributable to the sampling was calculated according to Gundersen and Jensen.[26] Errors ≤0.10 were accepted.

Cylinder test. Seven weeks after the surgery, animals injected with 1×10^{11} gc/ml rAAV5-shTH1 (n = 7), 3.4×10^{11} gc/ml rAAV5-shTH1scr (n = 9), as well as 6-OHDA- lesioned (n = 9) and intact (n = 6) control groups were subjected to a baseline cylinder test followed by a 6 mg/kg L-DOPA treatment. The animals were subjected to repeated cylinder tests 1, 3, and 6 hours after L-DOPA treatment to be able to follow the recovery period. The forelimb use in the cylinder test was adapted form the method described by Schallert and Tillerson and modified according to Kirik et al.[27,28] Briefly, the animals were allowed to move freely in a clear glass cylinder during video recording. Mirrors were placed behind the cylinder to be able to observe all forelimb contacts on the glass wall. The videotapes were evaluated by an observer blinded to the identity of the animals and the number of left and right paw touches on the cylinder wall were counted for at least 20 contacts.

Microdialysis surgery. The same animals that were subjected to the cylinder test were used for the biochemical measurements. A subset of these animals treated with 6-OHDA (n = 6), shTH1 (n = 4), shTH1scr (n = 4), and a nontreated intact group were used in a microdialysis experiment in order to assess the *in vivo* DOPA synthesis before the striatal sample collection. The rats were anesthesized with 12% isofluorane mixed with O_2 and N_2O and placed in a stereotaxic frame. The tooth bar was set to −2.3 mm. Microdialysis probes (Agnthos Microdialysis, Stockholm, Sweden) with 3-mm membrane length and 0.5-mm outer diameter, were used. With the help of a probe holder, they were inserted into the striatum at anterioposterior: +0.6 mm, mediolateral: −3.0 mm relative to bregma and dorsoventral: − 5.5 mm from the dural surface. The probes were connected to a syringe infusion pump (CMA/100; CMA/ Microdialysis, Solna, Sweden) via polyethylene tubing and perfused with normal ringer solution containing 145 mmol/l NaCl, 3 mmol/l KCl, and 1.3 mmol/l $CaCl_2$ at a constant rate of 2 µl/minute. After 1 hour of equilibration, three baseline dialysate samples (15 minutes each) were collected. The animals were then intraperitoneally injected with 100 mg/kg of NSD-1015 to block AADC enzyme activity. The dialysate samples were collected every 15 minutes for another 90 minutes following the NSD-1015 treatment. An aliquot of 5 µl perchloric acid was added into each sample tube in order to prevent oxidization of the substrates. The probes were withdrawn at the end of the sampling and animals were sutured and kept in their cages to recover for another 10 days before decapitation. The samples were kept at −80 °C until they were analyzed by high-performance liquid chromatography (HPLC) for the DOPA content.

Biochemical assays. Animals were decapitated and their brains were removed. The brain was rinsed with an ice-cold saline solution and was placed on a brain slicer. The striatum was rapidly dissected from the slices, frozen on dry ice and kept at −80 °C until analysis. At the time of analysis striatal tissue samples were sonicated 5 ml/mg in ice-cold homogenization buffer (20 mmol/l Tris-acetate, pH 6.1) and centrifuged at 20,000g for 10 minutes at 4 °C. The supernatant was divided into two parts; one part was used for TH enzyme activity and the other part was used for AADC enzyme activity as described below. The midbrain samples from those animals were fixed in 4% paraformaldehyde overnight for immunohistochemical detection of viral transduction and treated as described above.

In vitro TH enzyme activity assay. TH enzyme activity was measured according to the method described by Reinhard *et al*.[29] Briefly, 10 µl sample was mixed with 65 µl of reaction solution [4 µg l [3,5-^{3}H] tyrosine (Amersham Biosciences, Fairfield, CT), 100 µl L-tyrosine (500 µmol/l; Sigma), 100 µl Tris -acetate (200 mmol/l, pH 6.1), 84 mg catalase (Sigma), and 688 µl dH_2O]. Twenty-five microliter cofactor tetrahydrobiopterin (0.6 mg/ml, dissolved in 3 mg/ml dithiothreitol; Sigma) was then added to the reaction mixture. The samples were incubated for 20 minutes at 37 °C. The reaction was terminated by adding 1 ml charcoal–HCl and centrifuged at 20,000g for 15 minutes. 100 µl of the supernatant was transferred into a scintillation vial and 5-ml scintillation liquid (Ultima-Gold; PerkinElmer, Waltham, MA) was added. The number of decays per minute was measured in a liquid scintillation counter (Beckman LS 6500; Beckman Coulter, Fullerton, CA) and the values were corrected for the protein content in each sample, which was performed by using Bio-Rad DC protein

assay kit (Bio-Rad, Sundbyberg, Sweden) according to the manufacturer's instructions. The activity of TH enzyme was expressed as number of decays per minute per mg protein and as % of intact side.

In vitro AADC enzyme activity assay. AADC enzyme activity assay is based on the measurement of the enzymatic formation of DA from L-DOPA by using HPLC.[30] Briefly, 50 µl homogenized tissue was added to 350 µl incubation mixture (total volume 400 µl, in final concentrations) containing 50 mmol/l sodium phosphate buffer (pH 7.2), 0.25 mmol/l L-DOPA, 0.01 mmol/l pyridoxal phosphate, 0.17 mmol/lascorbic acid, 0.1 mmol/l pargyline, 1 mmol/l 2β-mercaptoethanol, and 0.1 mmol/l EDTA. The samples were then incubated at 37 °C for 20 minutes. The reaction was terminated by adding 600 µl ice-cold 0.1 mol/l perchloric acid and the samples were centrifuged at 10,000g for 10 minutes. The supernatant was filtered through minispin filters for 10 minutes at 10,000g. The samples were then diluted 100-fold in 0.1 mol/l perchloric acid. DA accumulation was determined by HPLC.

HPLC analysis of DA and DOPA. DOPA accumulation after NSD-1015 treatment in the microdialysis samples as well as DA concentration in striatal tissue extracts in *in vitro* AADC enzyme activity samples were determined by HPLC. Briefly, 20 µl of each microdialysis sample and 10 µl of AADC enzyme activity sample were injected by a cooled Spark Midas autosampler (Spark Holland, Emmen, the Netherlands) into an ESA Coulochem III (Chelmsford, MA) coupled to an electrochemical detector set to a potential of +350 mV. The mobile phase (13.8 g/l Na_2HPO_4, 30 mg/l Na_2-EDTA, 250 mg/l sodium octyl sulphate, 10% methanol, pH 3.0) was delivered at a flow rate of 0.5 ml/minute to a reversed phase C18 column (particle size 3 µm, 4.0 mm × 100 mm; Chromtech, Idstein, Germany). The peaks were analyzed by using the Clarity Chromatographic Station (DataApex, Prague, Czech Republic). The amount of DOPA was expressed in pmol either for each sample collected for 15 minutes to demonstrate *in vivo* TH enzyme activity or as the DOPA synthesis rate as fmol between 0 and 90 minutes after NSD-1015 treatment. The activity of AADC enzyme was expressed as newly formed DA per mg protein and as % of intact side.

Statistical analysis. Statistical significance for the group comparisons for TH and VMAT2 immunohistochemical stainings was analyzed by using two-way factorial analysis of variance. The cylinder test results were analyzed using two-way repeated measures analysis of variance. All two-way designs were followed with post hoc comparisons using individual contrast analysis with Bonferroni correction. One-way analysis of variance test was performed to compare results from biochemical assays, followed by Tukey honestly significant differences post hoc test. Statistical significance was set at $P < 0.05$. The statistical analysis was performed using JMP Statistical software (version 5.0.1.2; SAS Institute, Cary, NC). All values in this study are presented as mean ± standard error of mean.

Supplementary material

Table S1. Stereological quantification of tyrosine hydroxylase (TH) and vesicular monoamine transporter-2 (VMAT2) positive cell numbers in rat substantia nigra unilaterally injected with rAAV5 vectors expressing shTH1, shTH1scr, shTH2, shTH2scr, and enhanced green fluorescent protein (GFP).

Acknowledgments

We acknowledge the financial support from the Swedish Research Council (2005-33X-14552-03A), the European Union Marie Curie Actions Research Training Network Program in Nervous System Repair (MRTN-CT-2003-504636)**,** and the NEUGENE program (HEALTH-F5-2008-222925), and the International Brain Research Organization. We thank Toufik Abbas-Terki and Jolanta Sculz for design of the siRNA sequences; Stephan Hermening, Björn Anzelius, Biljana Georgievska, and Christina Isacsson for production of viral vectors; Helene Hall for enzyme activity assays, Siri Malmgren, Anneli Josefsson, Ulla Jarl**,** and Ulrika Sparrhult-Björk for technical support**;** and Bernard Schneider for his help in preparing the manuscript.

References

1. Scherer LJ, Rossi JJ. Approaches for the sequence-specific knockdown of mRNA. Nat Biotechnol 2003; 21(12): 1457-1465.
2. Meister G, Tuschl T. Mechanisms of gene silencing by double-stranded RNA. Nature 2004; 431(7006): 343-349.
3. Isacson R, Kull B, Salmi P, Wahlestedt C. Lack of efficacy of 'naked' small interfering RNA applied directly to rat brain. Acta Physiol Scand 2003; 179(2): 173-177.
4. Xia H, Mao Q, Paulson HL, Davidson BL. siRNA-mediated gene silencing in vitro and in vivo. Nat Biotechnol 2002; 20(10): 1006-1010.
5. Hommel JD, Sears RM, Georgescu D, Simmons DL, DiLeone RJ. Local gene knockdown in the brain using viral-mediated RNA interference. Nat Med 2003; 9(12): 1539-1544.
6. Xia H, Mao Q, Eliason SL, Harper SQ, Martins IH, Orr HT et al. RNAi suppresses polyglutamine-induced neurodegeneration in a model of spinocerebellar ataxia. Nat Med 2004; 10(8): 816-820.
7. Ralph GS, Radcliffe PA, Day DM, Carthy JM, Leroux MA, Lee DC et al. Silencing mutant SOD1 using RNAi protects against neurodegeneration and extends survival in an ALS model. Nat Med 2005; 11(4): 429-433.
8. Raoul C, Abbas-Terki T, Bensadoun JC, Guillot S, Haase G, Szulc J et al. Lentiviral-mediated silencing of SOD1 through RNA interference retards disease onset and progression in a mouse model of ALS. Nat Med 2005; 11(4): 423-428.
9. Grimm D, Streetz KL, Jopling CL, Storm TA, Pandey K, Davis CR et al. Fatality in mice due to oversaturation of cellular microRNA/short hairpin RNA pathways. Nature 2006; 441(7092): 537-541.
10. McBride JL, Boudreau RL, Harper SQ, Staber PD, Monteys AM, Martins I et al. Artificial miRNAs mitigate shRNA-mediated toxicity in the brain: implications for the therapeutic development of RNAi. Proc Natl Acad Sci U S A 2008; 105(15): 5868-5873.
11. Elbashir SM, Lendeckel W, Tuschl T. RNA interference is mediated by 21- and 22-nucleotide RNAs. Genes Dev 2001; 15(2): 188-200.
12. Harper SQ, Staber PD, He X, Eliason SL, Martins IH, Mao Q et al. RNA interference improves motor and neuropathological abnormalities in a Huntington's disease mouse model. Proc Natl Acad Sci U S A 2005; 102(16): 5820-5825.
13. Rodriguez-Lebron E, Denovan-Wright EM, Nash K, Lewin AS, Mandel RJ. Intrastriatal rAAV-mediated delivery of anti-huntingtin shRNAs induces partial reversal of disease progression in R6/1 Huntington's disease transgenic mice. Mol Ther 2005; 12(4): 618-633.
14. Alves S, Nascimento-Ferreira I, Auregan G, Hassig R, Dufour N, Brouillet E et al. Allele-specific RNA silencing of mutant ataxin-3 mediates neuroprotection in a rat model of Machado-Joseph disease. PLoS ONE 2008; 3(10): e3341.
15. Musatov S, Chen W, Pfaff DW, Kaplitt MG, Ogawa S. RNAi-mediated silencing of estrogen receptor {alpha} in the ventromedial nucleus of hypothalamus abolishes female sexual behaviors. Proc Natl Acad Sci U S A 2006; 103(27): 10456-10460.
16. Musatov S, Chen W, Pfaff DW, Mobbs CV, Yang XJ, Clegg DJ et al. Silencing of estrogen

receptor alpha in the ventromedial nucleus of hypothalamus leads to metabolic syndrome. Proc Natl Acad Sci U S A 2007; 104(7): 2501-2506.

17. Garza JC, Kim CS, Liu J, Zhang W, Lu XY. Adeno-associated virus-mediated knockdown of melanocortin-4 receptor in the paraventricular nucleus of the hypothalamus promotes high-fat diet-induced hyperphagia and obesity. J Endocrinol 2008; 197(3): 471-482.

18. Bahi A, Boyer F, Kolira M, Dreyer JL. In vivo gene silencing of CD81 by lentiviral expression of small interference RNAs suppresses cocaine-induced behaviour. J Neurochem 2005; 92(5): 1243-1255.

19. Hommel JD, Trinko R, Sears RM, Georgescu D, Liu ZW, Gao XB et al. Leptin receptor signaling in midbrain dopamine neurons regulates feeding. Neuron 2006; 51(6): 801-810.

20. Denovan-Wright EM, Rodriguez-Lebron E, Lewin AS, Mandel RJ. Unexpected off-targeting effects of anti-huntingtin ribozymes and siRNA in vivo. Neurobiol Dis 2008; 29(3): 446-455.

21. Zolotukhin S, Byrne BJ, Mason E, Zolotukhin I, Potter M, Chesnut K et al. Recombinant adeno-associated virus purification using novel methods improves infectious titer and yield. Gene Ther 1999; 6(6): 973-985.

22. Grimm D. Production methods for gene transfer vectors based on adeno-associated virus serotypes. Methods 2002; 28(2): 146-157.

23. Paxinos G, Watson C. The rat brain in stereotaxic coordinates, 2 edn. Academic Press: London, 2007.

24. West MJ. Stereological methods for estimating the total number of neurons and synapses: issues of precision and bias. Trends Neurosci 1999; 22(2): 51-61.

25. Torres EM, Meldrum A, Kirik D, Dunnett SB. An investigation of the problem of two-layered immunohistochemical staining in paraformaldehyde fixed sections. J Neurosci Methods 2006; 158(1): 64-74.

26. Gundersen HJ, Jensen EB. The efficiency of systematic sampling in stereology and its prediction. J Microsc 1987; 147(Pt 3): 229-263.

27. Schallert T, Tillerson JL. Intervention strategies for degeneration of dopamine neurons in parkinsonism: Optimizing behavioral assessment of outcome. In: Emerich DF, III RLD, Sanberg PR (eds). Central Nervous System Diseases. Humana Press: Totowa, NJ, 2000. , pp 131-151.

28. Kirik D, Rosenblad C, Bjorklund A, Mandel RJ. Long-term rAAV-mediated gene transfer of GDNF in the rat Parkinson's model: intrastriatal but not intranigral transduction promotes functional regeneration in the lesioned nigrostriatal system. J Neurosci 2000; 20(12): 4686-4700.

29. Reinhard JF, Jr., Smith GK, Nichol CA. A rapid and sensitive assay for tyrosine-3-monooxygenase based upon the release of 3H2O and adsorption of [3H]-tyrosine by charcoal. Life Sci 1986; 39(23): 2185-2189.

30. Nagatsu T, Yamamoto T, Kato T. A new and highly sensitive voltammetric assay for aromatic L-amino acid decarboxylase activity by high-performance liquid chromatography. Anal Biochem 1979; 100(1): 160-165.

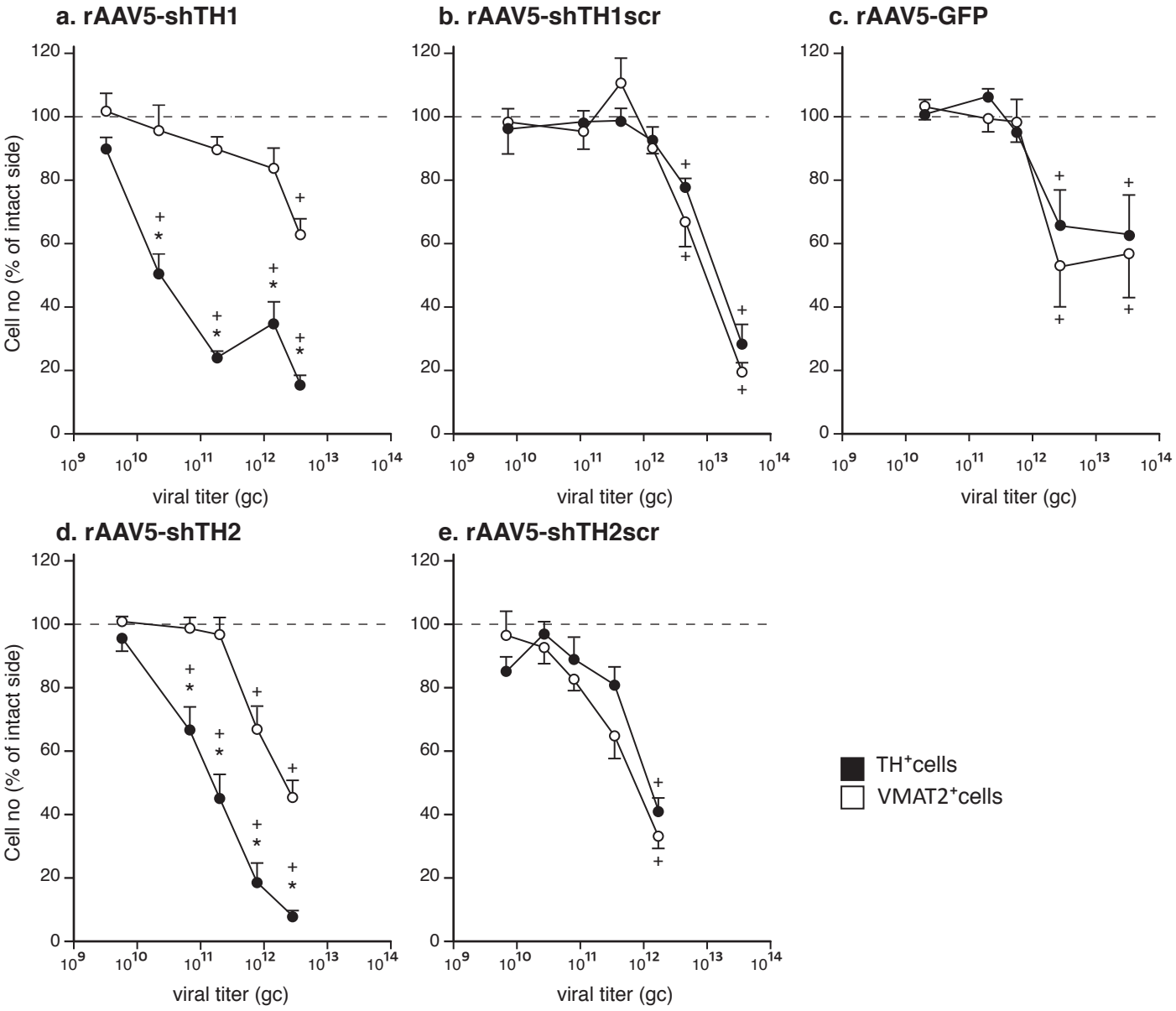

Figure 1 Stereological quantification of TH⁺ and VMAT2⁺ cell numbers in the substantia nigra. Estimations for animals injected with rAAV5 vectors encoding for (a) shTH1, (b) shTH1scr, (c) the GFP control protein (d) shTH2 or (e) shTH2scr are expressed as percent of intact (uninjected) side. Several dilutions of each vector stock (2-3 orders of magnitude) were analyzed in separate groups (n = 4-5 animals/titer/vector). Statistical comparisons were performed using two-way factorial ANOVA (a, $F(9,59) = 30.79$, $p<0.0001$; b, $F(11,59) = 38.59$, $p<0.0001$; c, $F(9,45) = 6.91$, $p<0.0001$; d, $F(11,63) = 24.26$, $p<0.0001$; e, $F(9,45) = 18.06$, $p<0.0001$), when significant followed by individual contrast post-hoc analysis with Bonferroni correction. *TH-positive cells different from the corresponding VMAT2+ cells in the same group. ⁺Different from the lowest titer group for the same phenotypic marker.

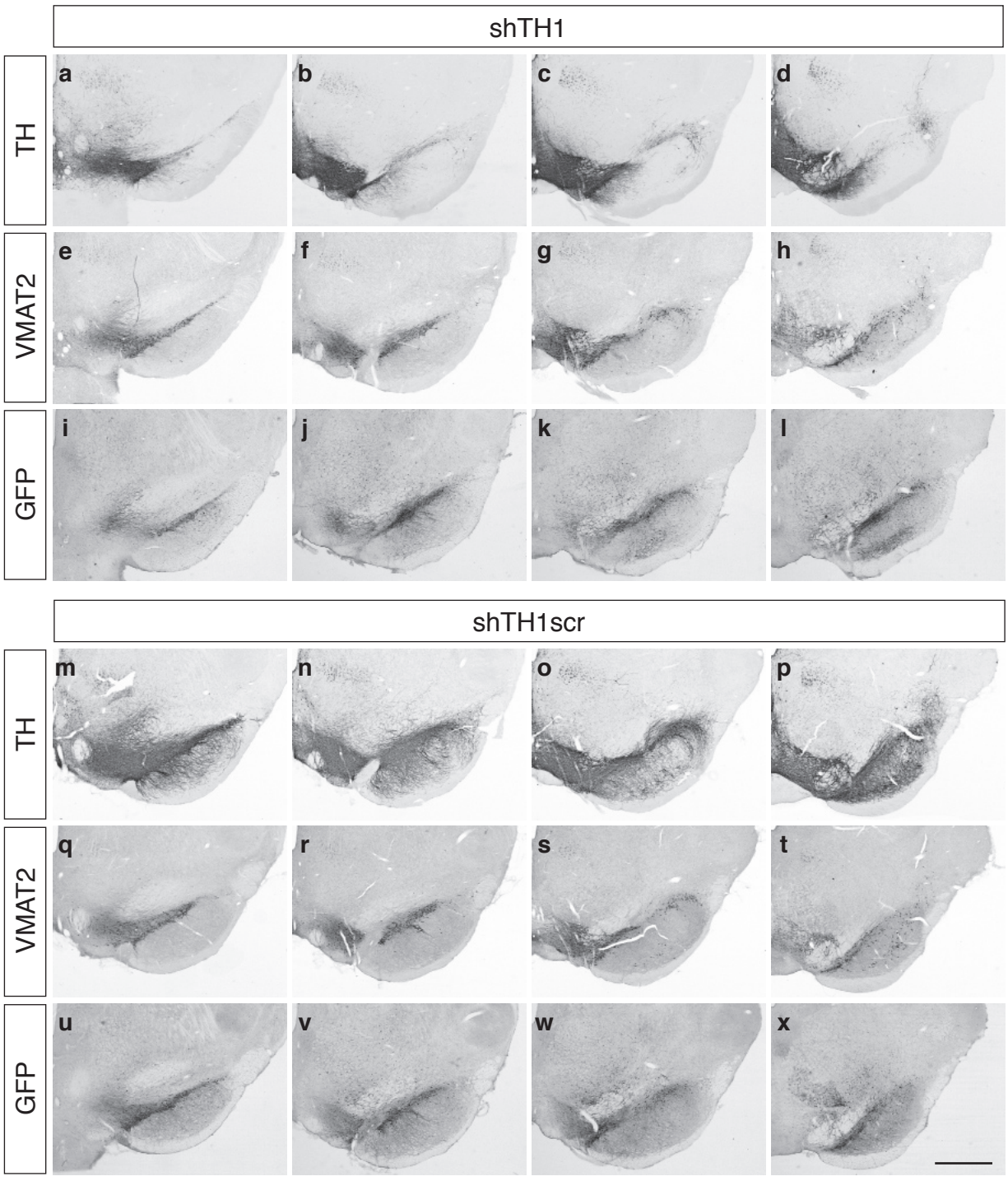

Figure 2 Serial sections from two representative animals injected woth rAAV5 encoding for shTH1 or shTH1scr. Midbrain sections were stained for TH (a-d, m-p), VMAT2 (e-h, q-t), or the GFP (i-l, u-x) proteins for both shTH1 (a-l) and shTH1scr (m-x) groups. The expression of the TH protein is knocked down by the expression of shTH1 construct (compare a-d with m-p), whereas the expression of the VMAT2 protein remains unaltered by both the active construct (e-h) and the scrambled control (q-t). Note that both vectors also express the GFP control gene for demonstration of transgene expression. As illustrated in panels i-l and u-x, the rAAV5 vectors used here provide robust expression in the ventral midbrain covering the entire substantia nigra. The titers of vectors (genome copies) illustrated in this figure are rAAV5-GFP: 2.0 x 10^{11}; rAAV5-shTH1: 1.8 x 10^{11}, rAAV5-shTH1scr: 4.4 x 10^{11}. Photomicrographs in each row represent 4 coronal views from anterior to posterior midbrain. Scale bar in x represents 500 µm and applies to all panels.

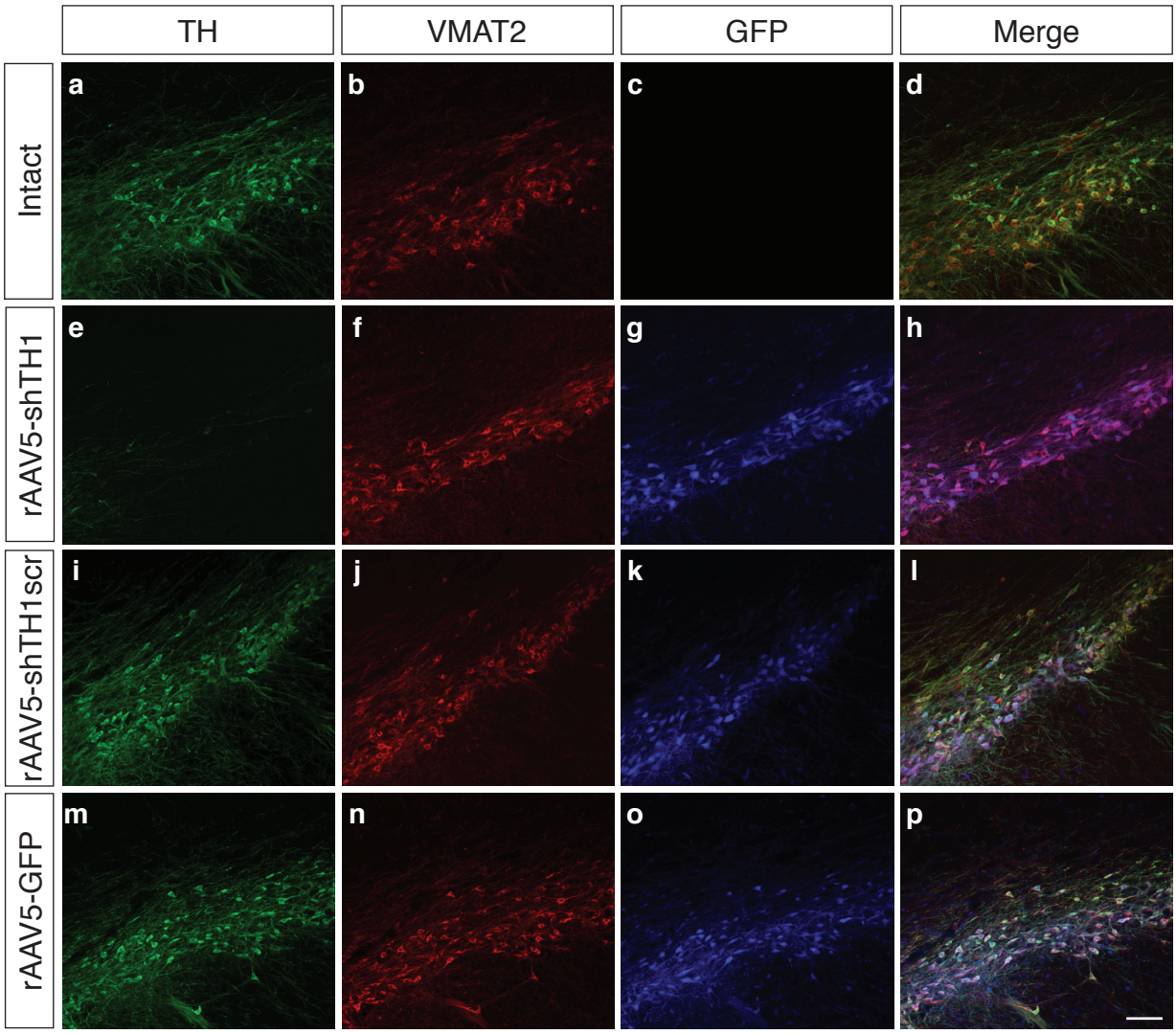

Figure 3 Triple immunohistochemical staining of substantia nigra injected with rAAV5 vectors with low 10^{11} gc/ml titers. Confocal microscopical images demonstrates labeling for the TH (green; panels a,e,i,m), VMAT2 (red; panels b,f,j,n) and the GFP (blue; c,g,k,o) proteins and the merged panels (d,h,l,p) on the (a-d) intact side, (e-h) rAAV5-shTH1, rAAV5-shTH1scr (i-l) or the (m-p) rAAV5-GFP vector injected sides. Note that both shTH1 and shTH1scr constructs also contain the GFP gene to allow for demonstration of transgene expression. rAAV5-shTH1 overexpression leads to a specific and efficient downregulation of the (e) TH protein, whereas in the rAAV5-shTH1scr or the rAAV5-GFP groups all three proteins are readily detectable giving the white color in the merged panels (l,p). The titers of vectors (genome copies) illustrated in this figure are rAAV5-GFP: 2.0 x 10^{11}; rAAV5-shTH1: 1.8 x 10^{11}, rAAV5-shTH1scr: 4.4 x 10^{11}. Scale bar in p represents 100 µm and applies to all panels.

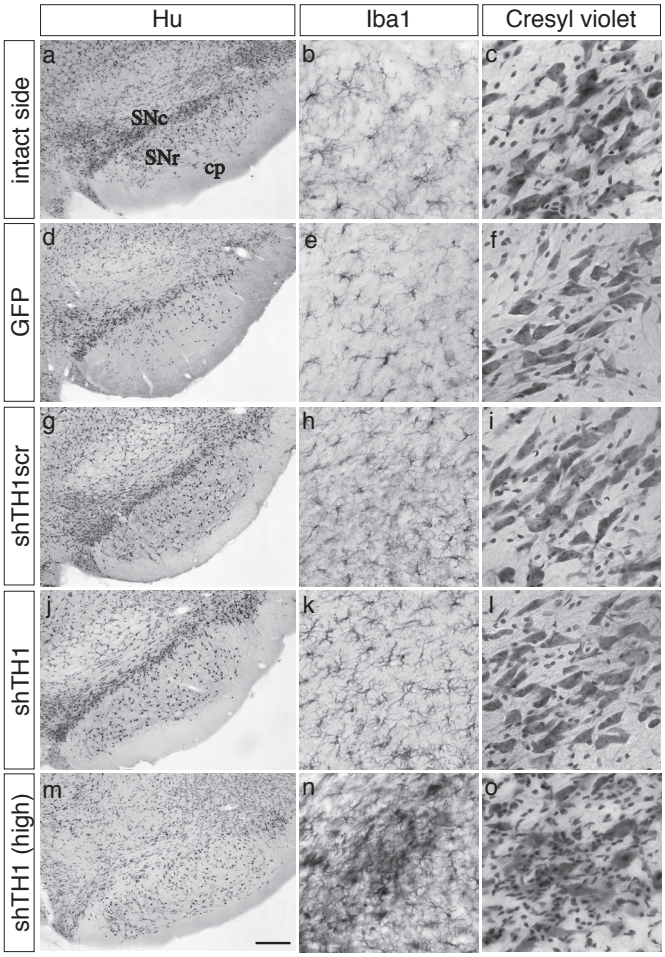

Figure 4 Low 10^{11} gc/ml titers of rAAV5 vectors coding for shTH1, shTH1scr or GFP proteins do not cause cytotoxicity. Photomicrographs demonstrates the neuronal Hu (a, d, g, j, m), microglial Iba1 (b, e, h, k, n), and the cresyl violet (c, f, i, l, o) stained specimens at the level of ventral midbrain. The cytoarchitectural integrity was maintained in animals treated with efficient dose of the viral preparations that did not lead to any toxicity (d-f for GFP, g-I for shTH1scr and j-l for shTH1 groups). There were no detectable differences between these specimens and the uninfected control side (a-c). On the other hand, injections of higher doses were associated with clearance of the neuronal cell layers within the (m) SN pars compacta, (n) activation of microglia and (o) hypercellularity suggesting a strong inflammatory response to toxicity. Note that the latter case is illustrated by a specimen from an animal treated with rAAV5-shTH1 vector but similar results were seen virtually all vectors at the toxic dose level. Scale bar in m represents 300µm in a, d, g, j and m, and 50 µm in all other panels, Abbreviations: cp, cerebral peduncle; SNc, substantia nigra pars compacta; SNr, substantia nigra pars reticulata.

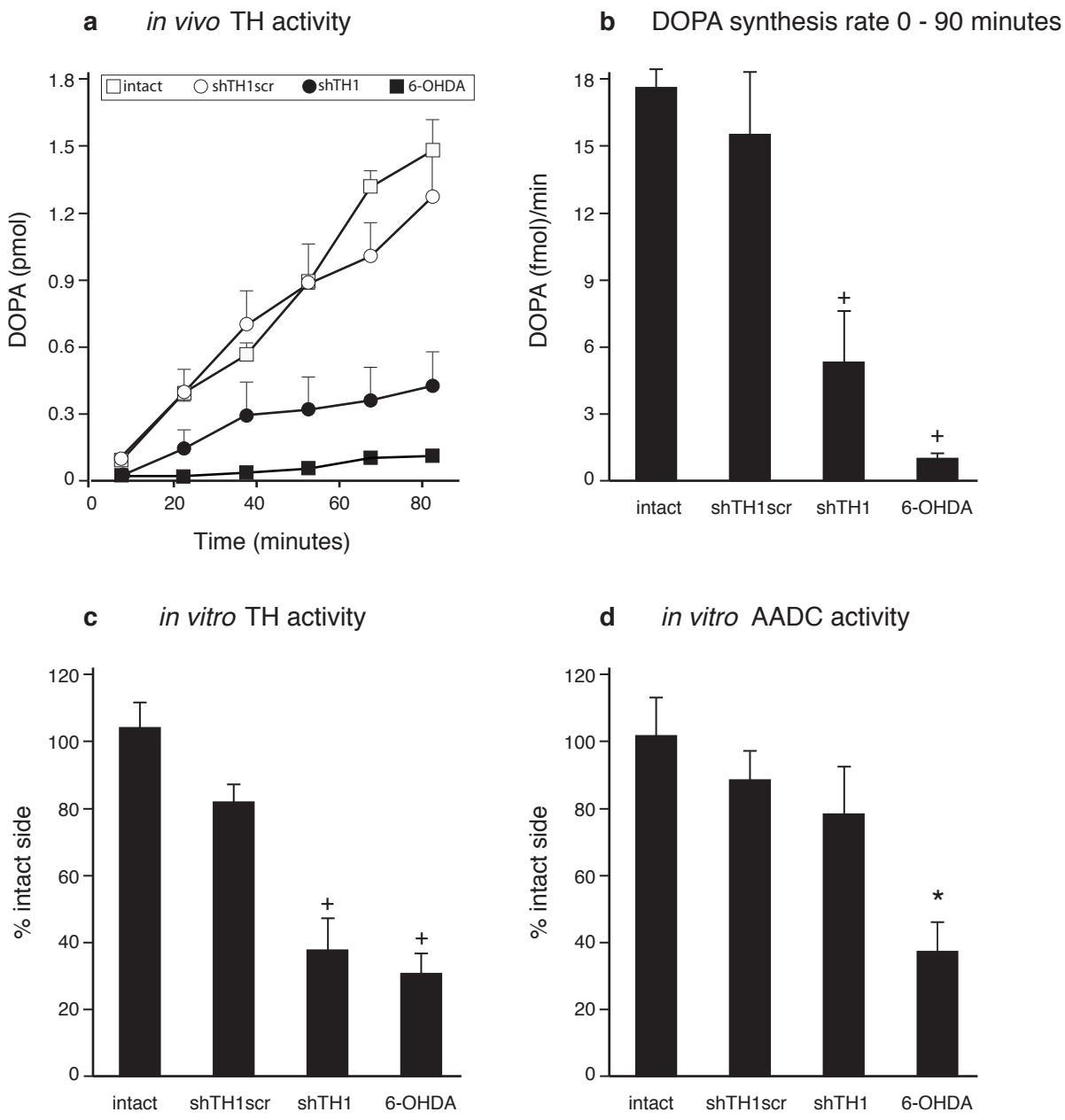

Figure 5 Biochemical alterations after rAAV5-shTH1 mediated TH knockdown. (a, b) DOPA accumulation was measured in the microdialysate after injection of 100mg/kg NSD-1015 at 9-12 weeks after the transduction. This assay provides a measure of the activity of TH enzyme in vivo. DOPA accumulation rate was significantly lower in shTH1 and 6-OHDA groups compared to the intact animals, whereas no significant difference was observed in shTH1scr group. Total DOPA synthesis measured over the 90 min sampling time in rAAV-shTH1 treated and 6-OHDA lesioned animals were significantly reduced as compared with the scrambled and intact controls (b). In a separate set of animals the striatal tissue homogenates were processed for in vitro enzyme activity. The results confirmed that TH activity was reduced by about 63% in shTH1 group and 70% in the 6-OHDA lesion group compared to the intact side. Whereas the scrambled controls did not differ from the intact controls. (c) AADC enzyme activity was similarly reduced in the 6-OHDA lesion group but remained unchanged in shTH1 and shTH1scr groups compared untreated animals, confirming the specificity of the knockdown (d). Statistical comparisons were performed using one-way ANOVA (b, $F(3,17) = 24.37$, $p<0.0001$; c, $F(3,29) = 23.47$, $p<0.0001$; d, $F(3,29) = 9,11$, $p<0.0003$), followed by Tukey post-hoc analysis. $^{+}$Different from intact control and shTH1scr groups. *Different from the all other groups.

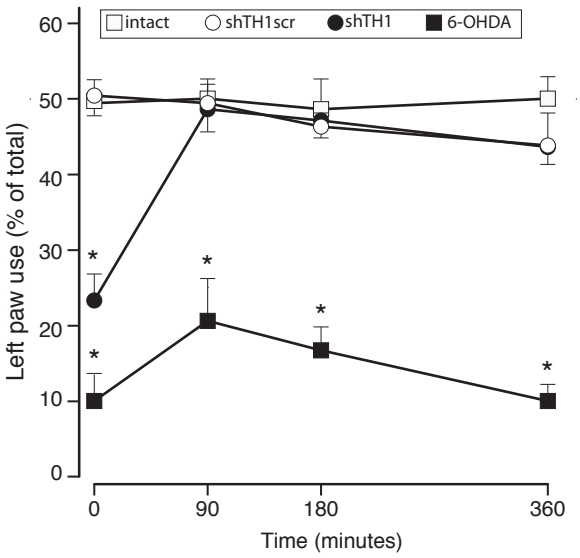

Figure 6 Long-term behavioral alterations in animals injected with 1 x 10^{11} gc/ml rAAV5-shTH1. Seven weeks after injection of the viral vectors, the animals were tested for forelimb motor performance using the cylinder test. Under baseline conditions (time 0 in figure), the left (affected) forepaw use was reduced to 23% in the shTH1 group, whereas the expression of the shTH1scr construct had no effect. These rats were able to use both forepaws symmetrically as seen in the intact rats (i.e., 50% of all touches were made with left forepaw). A fourth group of rats with intrastriatal 6-OHDA lesion was included as a lesion-reference group, which showed a clear impairment in this test and used the left forepaw only in 10% of the wall touches. Injection of L-DOPA (6 mg/kg) resulted in a complete recovery in the shTH1 group at already 90 minutes, which was maintained for at least 6 hours. The same dose of L-DOPA provided a minor change form (10% to 21%) in the 6-OHDA lesioned rats at 90 minutes. This effect was lost already at 180 minutes. *Different from the intact group at that time point. Statistical comparisons were performed using two-way repeated measures ANOVA, $F(3,26) = 7.40$, $p<0.0001$, followed by individual contrast post hoc analysis.

DOI: (MT.2009.142) Ulusoy A. et al. (2009) “Dose optimization for long-term rAAV-mediated RNA interference in the nigrostriatal projection neurons”

Stereological quantification of tyrosine hydroxylase (TH) and vesicular monoamine transporter 2 (VMAT-2) positive cell numbers in rat substantia nigra unilaterally injected with rAAV5 vectors expressing shTH1, shTH1scr, shTH2, shTH2scr and enhanced green fluorescent protein (GFP).

		TH		VMAT-2	
Group	Titer (gc/ml)	intact	injected	intact	injected
shTH1	3,7E+12	14507	2476	11400	10800
shTH1	3,7E+12	11772	2430	8100	3870
shTH1	3,7E+12	14364	2354	12180	9900
shTH1	3,7E+12	15012	1308	11700	5760
shTH1	3,7E+12	16524	1392	10750	6360
shTH1	3,7E+12	12289	2194	12360	7440
shTH1	3,7E+12	10195	1701	11440	6960
shTH1	3,7E+12	11491	3456	12960	7920
shTH1	3,7E+12	13738	1393	14800	8640
shTH1	3,7E+12	12787	767	12960	7160
shTH1	1,4E+12	14918	6172	13920	10980
shTH1	1,4E+12	15007	8325	16200	11760
shTH1	1,4E+12	15007	5395	15360	10800
shTH1	1,4E+12	16073	5106	12160	12400
shTH1	1,4E+12	15806	2081	12640	12000
shTH1	1,8E+11	13134	3233	12780	11580
shTH1	1,8E+11	14784	2946	13380	13320
shTH1	1,8E+11	12342	3960	13080	11700
shTH1	1,8E+11	11880	2277	12660	10020
shTH1	2,2E+10	14388	4963	14040	10380
shTH1	2,2E+10	14586	9042	10320	13440
shTH1	2,2E+10	13200	5742	12840	13020
shTH1	3,2E+09	15910	7322	15680	12800
shTH1	3,2E+09	16182	12204	14640	14240
shTH1	3,2E+09	16814	6916	11520	10320
shTH1	3,2E+09	14124	13992	14640	15420
shTH1	3,2E+09	13398	11352	13260	14280
shTH1	3,2E+09	14058	11484	9480	8100
shTH1	3,2E+09	14388	13398	12300	13320
shTH1scr	3,6E+13	13306	5616	14960	8256
shTH1scr	3,6E+13	11578	2448	12720	1032
shTH1scr	3,6E+13	11232	154	13920	323
shTH1scr	3,6E+13	12010	1474	12480	1296
shTH1scr	3,6E+13	12614	3292	11520	1830
shTH1scr	3,6E+13	12903	4002	11400	2508
shTH1scr	3,6E+13	12558	4727	11340	1840
shTH1scr	3,6E+13	12144	3381	12780	2220
shTH1scr	3,6E+13	14007	7797	11760	3340
shTH1scr	4,6E+12	13455	10350	11760	9060
shTH1scr	4,6E+12	15525	9384	12720	7020
shTH1scr	4,6E+12	12282	10488	11820	9600
shTH1scr	4,6E+12	12903	9453	12900	6930
shTH1scr	1,4E+12	13041	11109	13260	11520
shTH1scr	1,4E+12	13179	12972	10680	10140
shTH1scr	1,4E+12	13110	13179	13200	11520
shTH1scr	1,4E+12	11178	10488	10740	9720
shTH1scr	4,4E+11	15387	14835	10920	11940
shTH1scr	4,4E+11	15042	14490	14040	12660
shTH1scr	4,4E+11	14214	13179	11580	13500
shTH1scr	4,4E+11	14559	15870	10500	13320
shTH1scr	1,1E+11	12489	11730	12000	10980
shTH1scr	1,1E+11	12006	12558	11160	9060
shTH1scr	1,1E+11	12972	13179	14040	13860
shTH1scr	1,1E+11	12834	11937	11310	12570
shTH1scr	1,1E+11	11178	11109	11760	9780
shTH1scr	6,6E+09	14697	17251	11580	10860
shTH1scr	6,6E+09	14973	12834	11460	11760
shTH1scr	6,6E+09	14433	14088	12600	11220
shTH1scr	6,6E+09	14007	12144	11700	12600

		TH		VMAT-2	
Group	Titer (gc/ml)	intact	injected	intact	injected
shTH2	2,8E+12	13732	1972	12199	5228
shTH2	2,8E+12	14227	590	10455	5155
shTH2	2,8E+12	17938	108	14145	2453
shTH2	2,8E+12	15464	1300	11421	6512
shTH2	2,8E+12	14252	1632	13354	7939
shTH2	7,8E+11	15840	3135	13920	5880
shTH2	7,8E+11	13398	499	13200	7740
shTH2	7,8E+11	14784	518	13500	5580
shTH2	7,8E+11	12936	5874	10560	9660
shTH2	7,8E+11	14982	968	14220	9900
shTH2	7,8E+11	14520	440	12960	8700
shTH2	7,8E+11	13794	6776	13620	13080
shTH2	7,8E+11	14190	2297	12060	8100
shTH2	2,0E+11	14982	1753	12660	9300
shTH2	2,0E+11	12342	8514	11940	12360
shTH2	2,0E+11	14652	1837	13280	10480
shTH2	2,0E+11	14190	7755	13980	12180
shTH2	2,0E+11	15096	8991	13280	13360
shTH2	2,0E+11	15895	6727	16160	15200
shTH2	2,0E+11	12787	4240	13520	12960
shTH2	2,0E+11	13409	9657	12240	14160
shTH2	2,0E+11	13054	6593	12320	14880
shTH2	6,7E+10	15540	8924	14080	12880
shTH2	6,7E+10	11633	10723	13440	13840
shTH2	6,7E+10	16073	9590	12640	11520
shTH2	6,7E+10	14918	8436	13120	14240
shTH2	6,7E+10	13320	11189	13680	13040
shTH2	5,7E+09	15007	12965	12000	12640
shTH2	5,7E+09	13764	11899	14320	14160
shTH2	5,7E+09	13231	14030	12960	13360
shTH2	5,7E+09	13586	13142	13520	13680
shTH2	5,7E+09	12077	12254	13440	12880
shTH2scr	2,0E+12	14830	6394	13440	5360
shTH2scr	2,0E+12	14386	6061	14480	4560
shTH2scr	2,0E+12	13675	7126	12800	5160
shTH2scr	2,0E+12	13942	5683	11920	4360
shTH2scr	2,0E+12	14119	3963	13840	2430
shTH2scr	3,5E+11	16073	11522	14240	7740
shTH2scr	3,5E+11	14208	13142	13200	8400
shTH2scr	3,5E+11	12698	8725	14720	8280
shTH2scr	3,5E+11	13231	11988	13600	11680
shTH2scr	8,0E+10	13498	9768	13040	10800
shTH2scr	8,0E+10	14652	13675	14320	13280
shTH2scr	8,0E+10	15185	14652	12640	10480
shTH2scr	8,0E+10	13142	14386	13600	11680
shTH2scr	8,0E+10	13675	9946	13600	9280
shTH2scr	2,7E+10	14208	15540	12400	11520
shTH2scr	2,7E+10	13942	12698	13760	10720
shTH2scr	2,7E+10	14474	12876	12000	12800
shTH2scr	2,7E+10	14030	14741	12160	11920
shTH2scr	2,7E+10	14386	12698	15440	13680
shTH2scr	6,7E+09	14918	13586	13040	11840
shTH2scr	6,7E+09	13586	11810	12560	13600
shTH2scr	6,7E+09	14474	13231	12080	13200
shTH2scr	6,7E+09	13320	9324	13840	10720

Supplementary table

DOI: (MT.2009.142) Ulusoy A. et al. (2009) “Dose optimization for long-term rAAV-mediated RNA interference in the nigrostriatal projection neurons”

Stereological quantification of tyrosine hydroxylase (TH) and vesicular monoamine transporter 2 (VMAT-2) positive cell numbers in rat substantia nigra unilaterally injected with rAAV5 vectors expressing shTH1, shTH1scr, shTH2, shTH2scr and enhanced green fluorescent protein (GFP).

		TH		VMAT-2	
Group	**Titer (gc/ml)**	**intact**	**injected**	**intact**	**injected**
GFP	3,3E+13	15362	5195	13120	3390
GFP	3,3E+13	14386	8059	12960	7480
GFP	3,3E+13	11722	10589	12400	10400
GFP	3,3E+13	11100	7826	13520	7920
GFP	2,7E+12	14030	12077	14320	11360
GFP	2,7E+12	12787	3263	10960	1163
GFP	2,7E+12	14208	8725	13520	5160
GFP	2,7E+12	11899	7493	12400	7280
GFP	2,7E+12	14208	12654	12400	9440
GFP	5,6E+11	12077	11899	10720	11840
GFP	5,6E+11	14741	13231	14800	13600
GFP	5,6E+11	12787	11366	10400	12240
GFP	5,6E+11	13320	12166	13520	11760
GFP	5,6E+11	14208	15096	14240	11920
GFP	2,0E+11	11899	13142	13120	14320
GFP	2,0E+11	15540	14741	14880	15040
GFP	2,0E+11	14119	14918	13120	14480
GFP	2,0E+11	13231	14386	14800	12880
GFP	2,0E+11	11988	13320	13840	12400
GFP	2,0E+10	13108	12385	10960	10640
GFP	2,0E+10	13198	13470	13200	13920
GFP	2,0E+10	12837	13018	14160	15040
GFP	2,0E+10	13741	14374	14560	15040